

Multi Degrees of Freedom Robust Magnetic Levitation Control of a Flexible Transport Mover with Disturbance Observer and State Feedback Control

Ahmet F. Bozkurt, Omer F. Guney, Kadir Erkan

*Department of Mechatronics Engineering, Yildiz Technical University, 34100, Istanbul, Turkey
(afbzkurt90@gmail.com, oguney@yildiz.edu.tr, kerkan@yildiz.edu.tr)*

Abstract: In this study, a flexible transportation mover, based on magnetic levitation (maglev) principle, which contains hybrid electromagnets and linear induction motors (LIM) is proposed. Magnetic levitation force and inclination torque characteristics of the mover are analyzed using 3D Finite Element Method (FEM). Dynamic models representing multi degrees of freedom (DoF) maglev motion characteristics of the mover are developed by using magnetic equivalent circuit approach in conjunction with FEM analysis results. The mover dynamics shows non-linear characteristics and are unstable from the point view of controllability. In order to address the issue of instability and to precisely control the levitation gap clearance of the mover, a state feedback integral (SFI) controller is designed for each DoF with centralized control approach. The SFI controller design is based on the pole assignment method; the controller poles are determined by applying canonical polynomial of Manabe. The mover includes only optical displacement sensors that measure the gap clearance of the associated magnet poles. Other states required in effective operation of the SFI control are estimated and integrated into the control loop by means of designing disturbance observer (DO). The disturbance observer is capable of estimating external disturbance and as well as parameter uncertainty into a unique total disturbance value. By properly scaling and feedforwarding this estimated total disturbance value, robust control of the gap clearance is achieved. The performance of the proposed control algorithm is experimentally compared with the I-PD (modified PID) controller. The experimental results have shown effectiveness of the proposed control algorithm even in unbalanced loading conditions for each DoF.

Keywords: centralized control, state feedback integral control, disturbance observer, electro-magnetic modeling, magnetic levitation, mechatronics.

1. INTRODUCTION

Magnetic levitation systems eliminate mechanical contact which is the source of problems such as friction, vibration, noise, lubrication, etc. Hence magnetically levitated systems can work with greater accuracy and precision than their mechanical contact counterparts. With these advantages, they find applications as a key technology in magnetic bearing systems, vibration isolation systems, contactless transport of steel plates, wind turbines and new generation maglev transport vehicles (Boldea, 2013; Amrhein et al., 2016; Bozkurt et al., 2015; Morishita et al., 1989).

Hybrid electromagnets formed by combining permanent magnets and electromagnets reduce considerably the energy losses and the size of maglev systems. In such maglev systems, the levitation bias force is mainly provided by permanent magnets while the air gap is dynamically stabilized and controlled by the electromagnets (Guney et al., 2017; Ertugrul et al., 2016; Erkan et al., 2011). U and E-shaped electromagnets, which are frequently used in maglev systems, have a single-axis motion capability. More than one electromagnet must be placed in the same base and be controlled simultaneously so that full redundant multiple DoF magnetic levitation can be achieved. In this paper, the maglev mover consisting of triple configuration of hybrid

electromagnets and linear motors has been proposed to obtain 3-DoF stable gap clearance control capability by means of properly exciting the coils of the associated hybrid electromagnets. Besides, in $x - y$ plane, 3-DoF motion of the mover is achieved by the LIMs. The structure and component configuration of the mover is shown in Fig. 1 and 2.

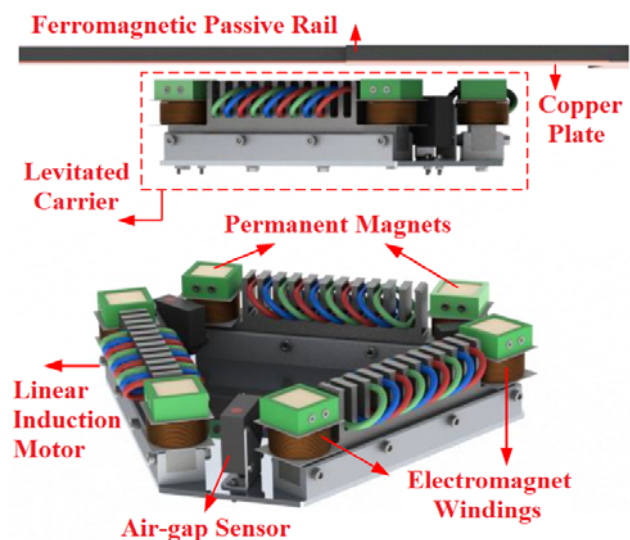


Fig. 1. The proposed maglev transporter system components.



Fig. 2. Levitating proposed system.

There are various systems in different studies available in the literature that are made up of configurations of linear induction motors and hybrid electromagnets that allow movement in 6 DoF (Ertuğrul et al., 2016; Erkan et al., 2007; Kim et al., 2013; Makino et al., 2004; Bucak et al., 2017). In these studies, it is necessary to install a linear synchronous motor which is defined as a stator along the guide line where the transportation is carried out. In the proposed system, the linear induction motors that provide the trust for linear motion are placed on the mover. Thus, the guide line part of the proposed system will be passive, simple and cost-effective because it will consist only of iron and copper plates. This allows for low-cost use in long-distance workplaces. In addition, the power consumption required for levitating of the relatively high weight (~15kg) mover is almost zero. If the amount of load to be carried increases, the capacity of the carrier can be increased in proportion to the dimensions of the hybrid magnets. Also in this study, a novel core design for linear motor is proposed. In literature, linear motor cores and hybrid electromagnet cores are separately designed and assembled on the mover plane (Bozkurt et al., 2015). This causes to increase in cost and size of the mover. However, the proposed core has both levitation coils and linear induction motor windings on itself. Using only 3 proposed cores, all 6 DoF motion can be achieved, which reduces the weight, the possibility of misalignment of the associated components with less efforts. FEM analysis and experimental results both show that using the same core to levitate and move along axis does not cause any error.

Several techniques such as PID control, fuzzy logic control and sliding mode control have been used in the literature to control the gap clearance of maglev devices (Choi et al., 2008; Kim et al., 2011; Liu et al., 2013; Narita et al., 2011; Matsumoto et al., 2014; Kubota et al., 2013; Sun et al., 2009; Yonezawa et al., 2014). In addition to the controllers, disturbance observer designs have been added to improve the system's control performance and as well as robustness under the external disturbances. Disturbance observer enhances robustness of the control system by feedforwarding the estimated disturbance input to the control loop by proper scaling (Baranowski et al., 2012; Gottzein et al., 1977 and 1980; Liu et al., 2002; Kim et al., 2001; Yang et al., 2007).

Guney et al., 2017 and Erkan et al., 2017; in their works, a modified type of PID, called as I-PD controller was designed for magnetically levitated steel-plate conveyance system and 4-pole hybrid electromagnet carrier system. In these studies, the experimental results of the I-PD control algorithm were presented. The experimental results are satisfactory but robustness under disturbances must be improved. In addition, the results of conventional PID controller show that there are excessive overshoots during position tracking which may cause undesirable results.

Numerical methods such as the finite element method are often used in field and loss analysis of motors and magnetic levitation systems. Ertuğrul et al., 2016 investigated numerically a 4-pole hybrid electromagnet levitated under the iron plate using the 3D FEM, and the force and inclination torque values were expressed in analytical equations. Kim et al., 2013 performed a detailed analysis of the linear motor interaction with the U-type hybrid electromagnet and the FEM results were compared with the model generated by the magnetic circuit approach. However, in this system the magnetic coupling effect on inclination torques was not demonstrated.

In this study, the electromagnetic attraction force characteristic of the hybrid electromagnet combined with linear induction motor is analyzed with 3D FEM (ANSYS Maxwell-3D). The analysis result revealed that energizing levitation coils of the hybrid electromagnet has no flux linkage on the linear motor core part of the associated hybrid electromagnet – linear motor core. Hence, the dynamics of the levitation can be separately modelled by means of magnetic equivalent circuit approach by just taking into account the structure of the hybrid electromagnet. The model for a single unit is non-linear in feature. To design the state feedback controllers from the point of view of linear control theory, linearized dynamics of each axis is developed under the assumption that gravity bias is provided by permanent magnets which stands for the coil current is zero around linearization point. SFI control is implementable in case of all states are available. In practice, however, not all state variables are measurable or sensor usage is avoided due to high cost. Here we propose that, only the air gap is measured and the other state variables are estimated using the disturbance observer. The centralized control topology based controlling of the global axis of each motion freedom is followed in design of SFI controllers by employing axis transformation matrix. Effectiveness of the modelling and SFI control approach is verified experimentally by comparing the results of I-PD controllers; previous study of the authors includes only simulation results for zero-power control algorithm (Bozkurt et al., 2015).

The main contributions of the paper are as follows:

- Proposal of a novel maglev mover consisting of triple configuration hybrid electromagnet and linear motor which are combined in a single core.
- Levitation modelling of the hybrid electromagnet and linear motor unit.
- Using centralized control topology, robust maglev control of the mover in 3 DoF with SFI and DO.

2. MODELING OF THE SYSTEM

The proposed system can move in 6 DoF which are:

- z axis: linear movement (air-gap)
- α axis: rotation around x axis (inclination)
- β axis: rotation around y axis (inclination)
- x axis: linear movement (plane)
- y axis: linear movement (plane)
- \mathcal{G} axis: rotation around z axis (plane).

The motions in the levitation mode are shown in Fig. 3. The control of the air gap at each pole is the main way by which the system can be stably operated and the active control can be performed. However, this decentralized approach makes the control of the angular axes (inclinations) very difficult due to omitting the inclination dynamics and results in the weakness against the disturbance inputs from associated directions. On the other hand, with the centralized approach, the problem is resolved by integrating inclination dynamics which are developed separately for each axis with coordinate transformations. These transformations are extracted from the geometrical configuration of the hybrid electromagnet and linear motor units as shown in Fig. 4.

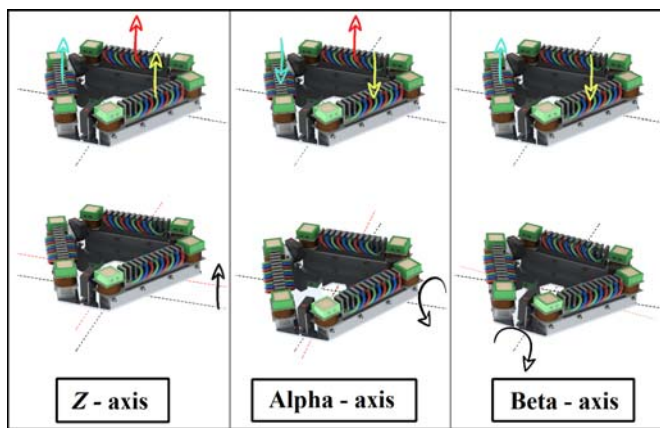


Fig. 3. Motions of the mover and representation of the attraction forces.

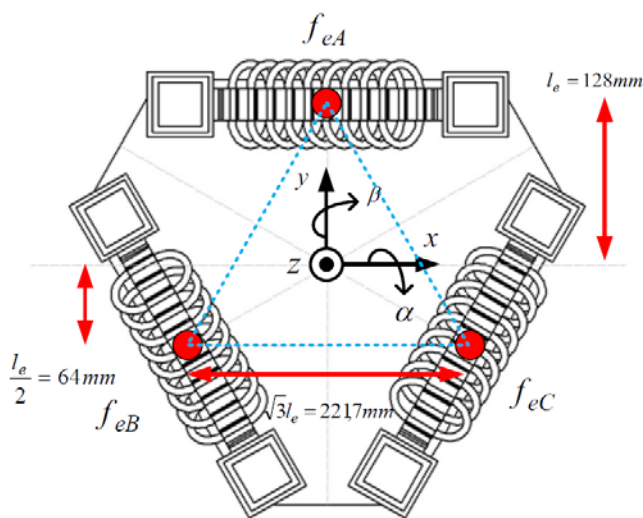


Fig. 4. Geometrical details of the mover.

The currents flowing through the associated electromagnets coil can be converted into virtual or global axis currents by using a current transformation matrix. In the same manner, gap clearances at the poles of the electromagnets can be converted into axial displacements. These transformation matrices can be written as follows:

$$\begin{bmatrix} \Delta i_z \\ \Delta i_\alpha \\ \Delta i_\beta \end{bmatrix} = \begin{bmatrix} 1/3 & 1/3 & 1/3 \\ 1 & -1/2 & -1/2 \\ 0 & \sqrt{3}/2 & -\sqrt{3}/2 \end{bmatrix} \begin{bmatrix} \Delta i_A \\ \Delta i_B \\ \Delta i_C \end{bmatrix} \quad (1)$$

$$\begin{bmatrix} \Delta z \\ \Delta \alpha \\ \Delta \beta \end{bmatrix} = \begin{bmatrix} -1/3 & -1/3 & -1/3 \\ -2/3l_e & 1/3l_e & 1/3l_e \\ 0 & -1/\sqrt{3}l_e & 1/\sqrt{3}l_e \end{bmatrix} \begin{bmatrix} \Delta x_A \\ \Delta x_B \\ \Delta x_C \end{bmatrix} \quad (2)$$

The electromagnetic attraction force characteristic of the hybrid electromagnet and linear motor unit beneath a passive rail have been analyzed using the finite element method. The 3D mesh structure used in the analysis of the core is demonstrated in Fig. 5. The flux distribution corresponding to the analysis is demonstrated when the gap clearance is 6 mm. The flux distribution is confined and concentrated on the path combining hybrid electromagnet poles of the unit. There is distinctly no flux fringing over the teeth and slot of linear motor part of the unit since the passive rail has relatively higher permeability than air. This results in the significant simplification that the hybrid electromagnet and the linear motor can be modelled in separate manner. Moreover, to develop an analytical model for the attraction force of the hybrid electromagnet, magnetic equivalent circuit approach can be readily applied without loss of generality. Fig. 7 shows the variation of the z -axis electromagnetic attraction force characteristic depending on the z -axis gap clearance and the associated z -axis current. The characteristic is non-linear in feature as expected.

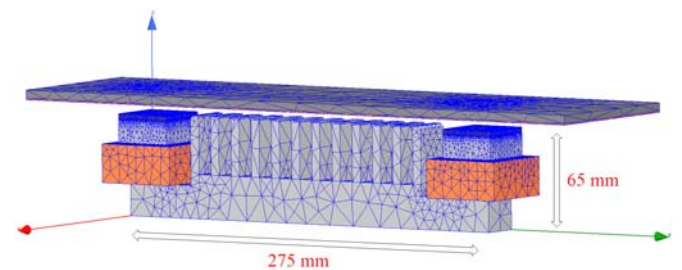


Fig. 5. Single hybrid levitation motor mesh structure.

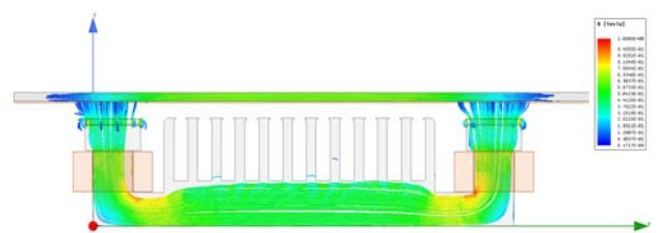


Fig. 6. Magnetic flux density stream on surface.

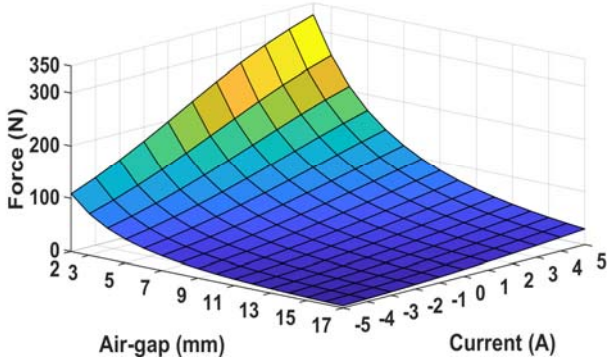


Fig. 7. FEM results of z -axis attraction force (single core).

The electromagnetic attraction force which is a non-linear function of the gap clearance (x) and the associated current (i) is obtained as in (3), by employing the well-established magnetic equivalent circuit analysis approach. Eq. (3) is an analytical description of the characteristic demonstrated in Fig. 7 and can be used to precisely model the attraction force by proper parametrization.

$$f_e(i, x) = \frac{\mu_0 N^2 S}{2} \left(\frac{i + i_{PM}}{x + l_{PM}} \right)^2 = k \left(\frac{i + i_{PM}}{x + l_{PM}} \right)^2 \quad (3)$$

where structural parameters representing the number of coil turns (N), permeability of air (μ_0) and etc. can be collected into a single parameter, k , in proper units to get a simplified expression.

Governing non-linear mechanical and electrical dynamics for a single unit can be described as:

$$m \frac{d^2 x}{dt^2} = -f_e(i, x) + mg + f_d \quad (4)$$

$$V = Ri + \frac{d\lambda}{dt} = Ri + \frac{\partial \lambda}{\partial i} \frac{di}{dt} + \frac{\partial \lambda}{\partial x} \frac{dx}{dt} \quad (5)$$

where g is the gravitational acceleration, m is the mass of the levitating part, f_d is the externally applied disturbance force, λ is the total flux linkage and Φ is the magnetic flux.

The nonlinear force equation is linearized for tiny deviations around a specified equilibrium point, (i_0, x_0), hence, the linear controller design can be performed easily;

$$f_{e0}(i_0, x_0) = k \left(\frac{i_0 + i_{PM}}{x_0 + l_{PM}} \right)^2 = mg \quad (6)$$

The linearized dynamics of the system can be expressed as:

$$m \frac{d^2 \Delta x}{dt^2} = K_x \Delta x - K_i \Delta i + f_d \quad (7)$$

$$K_x = - \left. \frac{\partial f_e}{\partial x} \right|_{\substack{i=i_0 \\ x=x_0}} \quad \& \quad K_i = \left. \frac{\partial f_e}{\partial i} \right|_{\substack{i=i_0 \\ x=x_0}} \quad (8)$$

$$\frac{di}{dt} = - \frac{R}{L} i + \frac{K_v}{L} \Delta x + \frac{1}{L} \Delta V \quad (9)$$

$$K_v = \left. \frac{\partial \lambda}{\partial x} \right|_{\substack{i=i_0 \\ x=x_0}} \quad \& \quad L = \left. \frac{\partial \lambda}{\partial i} \right|_{\substack{i=i_0 \\ x=x_0}} \quad (10)$$

where K_x and K_i are the gap and current stiffness coefficients and K_v is the coefficient of motion back-emf. If the state variables are selected as $\Delta z(t)$, $\Delta \dot{z}(t)$ and $\Delta i_z(t)$, the linear system model for 1-DoF obtained in a state-space form as follows:

$$\frac{d}{dt} \begin{pmatrix} \Delta x(t) \\ \Delta \dot{x}(t) \\ \Delta i(t) \end{pmatrix} = \begin{pmatrix} 0 & 1 & 0 \\ \frac{K_x}{m} & 0 & -\frac{K_i}{m} \\ 0 & \frac{K_v}{K_i} & -\frac{R}{L} \end{pmatrix} \begin{pmatrix} \Delta x(t) \\ \Delta \dot{x}(t) \\ \Delta i(t) \end{pmatrix} + \begin{pmatrix} 0 \\ 0 \\ \frac{1}{L} \end{pmatrix} \Delta V(t) + \begin{pmatrix} 0 \\ \frac{1}{m} \\ 0 \end{pmatrix} F_d(t)$$

$$\dot{x}(t) = Ax(t) + Bu(t) + EF_d(t) \quad (11)$$

The block diagram of the transfer function of the 1-DoF system is shown in Fig. 8:

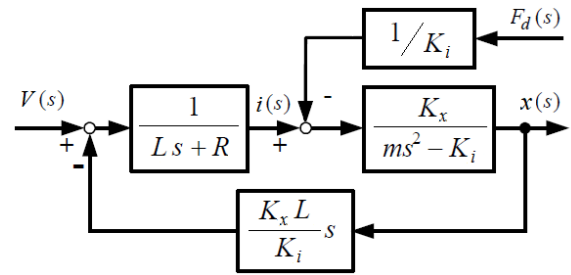


Fig. 8. Transfer function block diagram of the maglev system.

Linearized global governing mechanical dynamics according to the geometric placements of the electromagnets are expressed for 3 degrees of freedom as following;

$$M \frac{d^2 \Delta z}{dt^2} = 3K_x \Delta z + 3K_i \Delta i_z - F_{dz} \quad (12)$$

$$J_\alpha \frac{d^2 \Delta \alpha}{dt^2} = \frac{3}{2} l_e^2 K_x \Delta \alpha + l_e K_i \Delta i_\alpha - F_{d\alpha} \quad (13)$$

$$J_\beta \frac{d^2 \Delta \beta}{dt^2} = \frac{3}{2} l_e^2 K_x \Delta \beta + l_e K_i \Delta i_\beta - F_{d\beta} \quad (14)$$

3. CONTROLLER DESIGN

The linearized magnetic levitation dynamics stated by Eq. (11) is unstable in open loop. Therefore, feedback control algorithms that can stabilize the system must be applied. In the state-space model of the system, the eigenvalues of the matrix A represent the poles of the system. The zero – pole map of a representative system consistent with experimental setup is shown in Fig. 9. Instability of the system is detected from Fig. 9 since an unstable pole exists on the right side of imaginary s -plane.

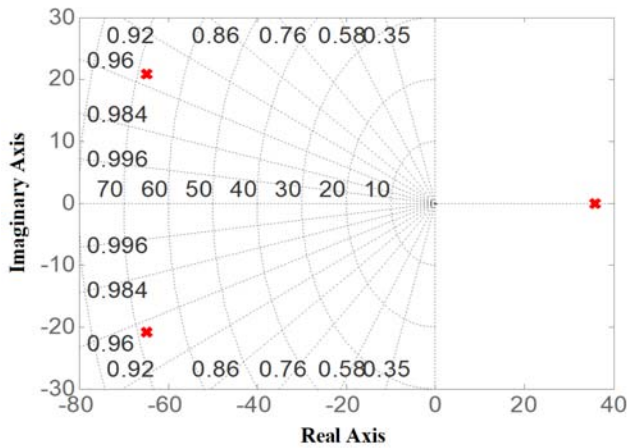


Fig. 9. Open-loop system poles shown in zero-pole map.

The centralized control approach, as mentioned in the electromagnetic analysis section, is based on the principle of individual control of each global axis with the assumption that they are independent of each other. Fig. 10 shows the structure of the 1-DoF controller in conjunction with a DO. Fig. 11 shows the overall control in 3-DoF by using the transformation matrices (gap clearance, Eq. (2), and the current, Eq. (1)) for SFI and DO approach. Independent controllers are designed for each axis (α , β and z).

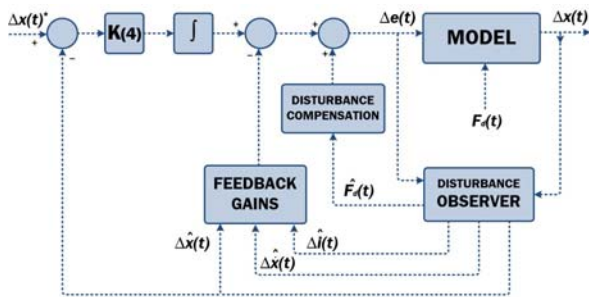


Fig. 10. SFI + Disturbance Observer Controller.

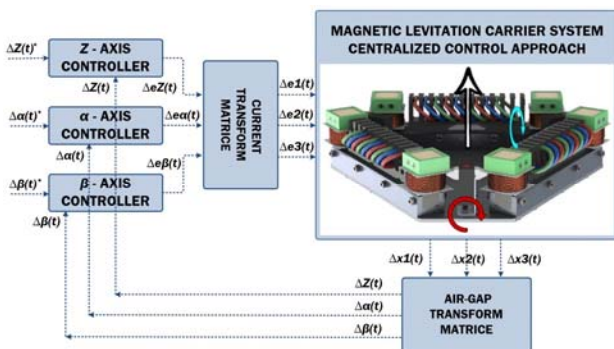


Fig. 11. Centralized control block diagram.

To converge the steady-state error of the output state variable to zero, the integral of this variable must be added as a state variable to the state-space equation (Barie et al., 1996), this is so called integral control. Moreover, the integral control can overcome the deviation from reference operating point and enhance robustness with respect to external disturbances. The integral term is added as a new state variable to the governing

system equation. As a result, the order of the governing system dynamics is increased by 1, which corresponds to an augmented system as expressed by Eq. (15);

$$\frac{d}{dt} \begin{bmatrix} \Delta z(t) \\ \Delta \dot{z}(t) \\ \Delta i_z(t) \\ \int [0 - \Delta z(t)] dt \end{bmatrix} = \begin{bmatrix} 0 & 1 & 0 & 0 \\ \frac{K_{yz}}{m} & 0 & \frac{K_{iz}}{m} & 0 \\ 0 & \frac{K_{yz}}{L_z} & \frac{R_z}{L_z} & 0 \\ -1 & 0 & 0 & 0 \end{bmatrix} \begin{bmatrix} \Delta z(t) \\ \Delta \dot{z}(t) \\ \Delta i_z(t) \\ \int [0 - \Delta z(t)] dt \end{bmatrix} + \frac{1}{L_z} \Delta V_z(t) \quad (15)$$

Canonical polynomial method is an effective method to decide the coefficients of the characteristic polynomial of single-input single-output systems. The basic idea behind this approach is to determine a suitable stable characteristic polynomial using time constant and stability indices. While the time constant affects the output response speed, the stability indices determine the output waveform with robustness and stability against parameter uncertainty (Manabe, 1998 & 2002).

The characteristic equation for 4th order closed loop control system is defined as follows:

$$P_4(s) = a_4 s^4 + a_3 s^3 + a_2 s^2 + a_1 s + a_0 \quad (16)$$

γ stability indices and the τ equivalent time constant are defined as follows:

$$\gamma_i = \frac{a_i^2}{a_{i+1} a_{i-1}} \quad (i = 1, 2, 3) \quad \& \quad \tau = \frac{a_1}{a_0} \quad (17)$$

Stability limits are determined as follows:

$$\gamma_i^* = \frac{1}{\gamma_{i+1}} + \frac{1}{\gamma_{i-1}} \quad (\gamma_n = \gamma_0 = \infty) \quad (18)$$

The Routh - Hurwitz stability analysis for polynomials at 3rd and 4th grades yields the following result:

$$\gamma_i > \gamma_i^* \quad (i = 1 \sim n - 1) \quad (19)$$

In the polynomials of rank 5 and above, stability is ensured by the following condition:

$$\gamma_i > 1.12 \gamma_i^* \quad (i = 1 \sim n - 1) \quad (20)$$

The canonical polynomial is described by (21) in terms of the time constant and the stability indices

$$P(s) = a_0 \cdot \left[\sum_{i=2}^n \left(\prod_{j=1}^{i-1} \frac{1}{\gamma_{j-1}^j} \right) (\tau \cdot s)^i \right] \cdot \tau \cdot s + 1 \quad (21)$$

In the 1960s, Kessler suggested that all gamma values should be 2 (two). Accordingly, in the 1980s, Manabe suggested that $\gamma_1 = 2.5$ and others as 2 (two) (Manabe, 1998 & 2002). For a maglev system, it is a practically acceptable approach by taking time constant of around 0.1 seconds. If the reference polynomial is solved by equating zero, 4 roots are obtained

where the system roots should be moved with the designed controller. The poles of the system at 4th order are found to be double roots at $-40 \pm 40j$ as taking time constant of 0.1s.

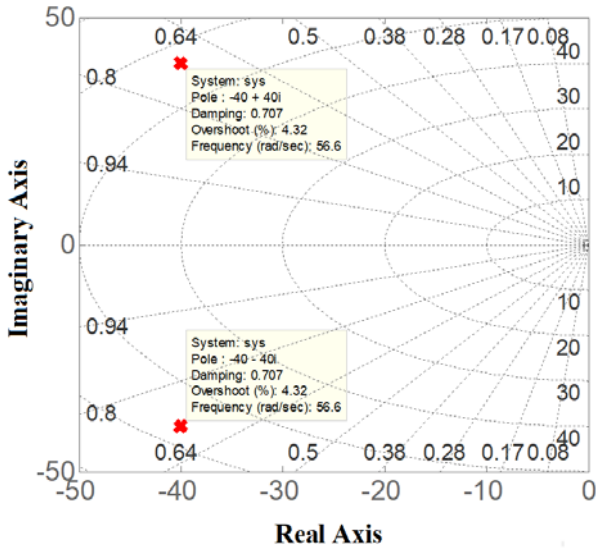


Fig. 12. Zero-pole map of the desired system.

In order to apply the pole assignment method, the augmented system must satisfy the controllability condition. Since the matrix A is full rank, the augmented system can be controlled and the pole assignment technique can be applied as well. In this study, pole assignments have been performed with the MATLAB program using “**place**” command as follows:

$$K = \text{place}(A, B, [p_1, p_2, p_3, p_4]) \quad (22)$$

State feedback gain matrix and integral gain can be expressed as follows:

$$K = [F_1 \quad -F_2] \quad (23)$$

Implementation of the state feedback control relies on the availability of the all state variables. However, in practical applications, some state variables are not directly measurable or the sensor usage is avoided because of the high cost. Usage of state observers is the frequent choice to overcome unavailable state measurement as well as to reduce the cost. In conventional linear observers in which the integration disturbance estimate is omitted, the precise observation and estimation of the states are violated in case of existing external disturbance excitation or model parameter uncertainty. Therefore, integration of disturbance estimate is a critical point of successful estimate and observation and even required to obtain stable operation. Besides, the estimated disturbance can be feedforwarded to the control loop by properly scaling so that the disturbance compensation can be achieved and as a result, robustness of the control is enhanced.

In disturbance observer design, the system model is expanded by adding disturbing force as a state variable. The disturbance input and other state variables of the system can be estimated accurately by the disturbance observer. In maglev systems, the disturbance acts like as a stepwise input.

Hence, the disturbance dynamic is modelled as a step function with all derivatives zero. Eq. (24) expresses the extended state space form for the system by inclusion of the disturbance as a state variable, addition of 4th line. In this paper it is assumed that only the gap clearances are available and measurable. Therefore, other state variables speed of the gap clearance change and the associated coil currents, are to be estimated accurately by the disturbance observer.

$$\frac{d}{dt} \begin{bmatrix} \Delta z(t) \\ \Delta \dot{z}(t) \\ \Delta i_z(t) \\ F_d \end{bmatrix} = \begin{bmatrix} 0 & 1 & 0 & 0 \\ \frac{K_{xz}}{M} & 0 & \frac{K_{iz}}{M} & \frac{1}{M} \\ 0 & \frac{K_{xz}}{K_{iz}} & \frac{R_z}{L_z} & 0 \\ 0 & 0 & 0 & 0 \end{bmatrix} \begin{bmatrix} \Delta z(t) \\ \Delta \dot{z}(t) \\ \Delta i_z(t) \\ F_d \end{bmatrix} + \begin{bmatrix} 0 \\ 0 \\ \frac{1}{L_z} \\ 0 \end{bmatrix} \Delta V_z(t) \quad (24)$$

$$\dot{x}_o = A_o x_o + B_o u$$

The disturbance dynamics is described in a compact form as follows:

$$\dot{\hat{x}}_o = A_o \hat{x}_o + B_o u + L(\Delta z - \Delta \hat{z}) \quad (25)$$

where L is the observer gain matrix which must be defined properly. In disturbance observer design, similar to the SFI controller design, the observer poles that will stabilize the extended system are assigned to desired dynamics which is consistent with the controller poles. The Kessler canonical form was used to assign observer poles as in controller design. However, the observer must be chosen to have 5-10 times faster dynamics than the controller's.

One of the benefit of applying disturbance observer is the robustness enhancement of the control by means of estimated disturbance compensation. In disturbance compensation, the estimated disturbance \hat{F}_d is scaled by a proper compensation coefficient and added to the control path as a correction term. In order to find the compensation coefficient, it is assumed that there is no dynamic effect in the steady-state:

$$t = \infty \quad \Delta z(\infty) = 0 \quad \Delta \dot{z}(\infty) = 0 \quad (26)$$

The state equations of the system can be written as:

$$0 = \begin{bmatrix} 0 & 1 & 0 \\ \frac{K_{xz}}{M} & 0 & \frac{K_{iz}}{M} \\ 0 & \frac{K_{xz}}{K_{iz}} & \frac{R_z}{L_z} \end{bmatrix} \begin{bmatrix} \Delta z(\infty) \\ \Delta \dot{z}(\infty) \\ \Delta i_z(\infty) \end{bmatrix} + \begin{bmatrix} 0 \\ 0 \\ \frac{1}{L_z} \end{bmatrix} \Delta V_z(\infty) + \begin{bmatrix} 0 \\ \frac{1}{M} \\ 0 \end{bmatrix} F_d \quad (27)$$

By arranging the state equation, it becomes:

$$\frac{K_{iz}}{M} \Delta i_z(\infty) - \frac{1}{M} F_d = 0 \quad (28)$$

$$-\frac{R_z}{L_z} \Delta i_z(\infty) + \frac{1}{L_z} \Delta V_z(\infty) = 0 \quad (29)$$

The disturbance compensation coefficient is obtained as follows by arranging these two equations:

$$K_{Fd} = \frac{\Delta V_z(\infty)}{F_d} = \frac{R_z}{K_{iz}} \quad (30)$$

4. RESULTS & DISCUSSION

An experimental test bench was constructed and the levitation photo is seen in Fig. 1. The bench parameters are tabulated in Table 1. Omron Z4W-V displacement sensors, LEM LTS6 current sensors were employed to measure the gap clearances and the currents. The controllers and observers were implemented in digital form by using MATLAB xPC target configuration. NI 6259 and 6733 DAQ cards were used to receive measurement signals from the sensors and to transmit the control signals to the power amplifiers. Signal flowchart of the bench is functionally demonstrated in Fig. 13. Programming of the all controllers were performed in Simulink environment by proper usage of the blocks.

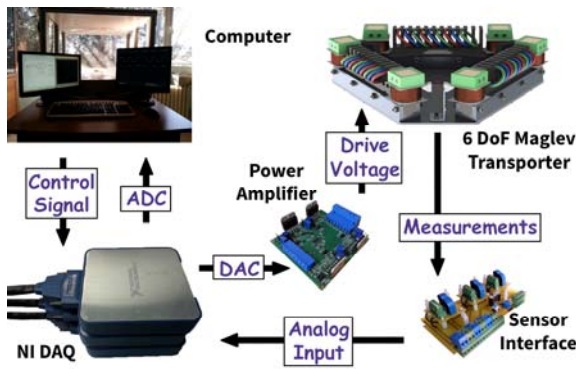


Fig. 13. The functional signal flowchart of the system.

Table 1. Experimental Setup Parameters.

Constant parameter	Value	Unit
Dimensions of the mover	41x37x42	cm
Dimensions of the PMs	35x35x3.5	mm
Current of the PMs	14.875	A
Mass of the mover	17	kg
Inertia for α and β axes	0.25	kg.m ²
K_{xz} (gap stiffness coefficient)	21305	N/m
K_{iz} (current stiffness coeff.)	22.4	N/A
Number of turns	200	Turns
Resistance of the coils	2.6	Ohms
Inductance of the coils	0.078	Henry

The linearization point for the nonlinear governing dynamic equations was chosen as ($x_0=9\text{mm}$ and $i_0=0\text{A}$) so that gravity was compensated by the permanent magnets. To evaluate and show the effectiveness of the proposed control approach, the experiments were conducted for I-PD controllers under the same conditions as with the proposed designs. In design of the I-PD controllers, the canonical polynomial approach was used as stated in reference (Erkan et al., 2017). The experiments are classified into two groups; in the first group, reference tracking performance was tested and in the second group disturbance compensation and rejection property was examined. Fig. 14 and 15 demonstrate $\pm 2\text{mm}$ step reference tracking response for z -axis displacement and the

corresponding current change. The proposed SFI controller and DO, surely shows better performance than I-PD counterpart in terms of maximum overshoot and settling time; furthermore the corresponding coil current is less oscillatory which means that high frequency current control is not needed and the system is sufficiently far from stability margin. Increment of reference amplitude has a tendency to violate the levitation stability since the undesired oscillation amplitude are amplified for I-PD controllers. Hence, I-PD controller can be operate relatively small reference change around the linearization point. The existing reference signal is increased by 1 mm and I-PD controller has shown unacceptable performance with time to time instability while the proposed approach has an acceptable performance.

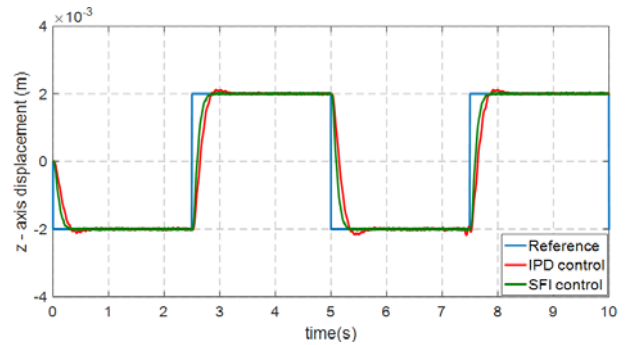


Fig. 14. $\pm 2\text{mm}$ reference tracking (Z axis).

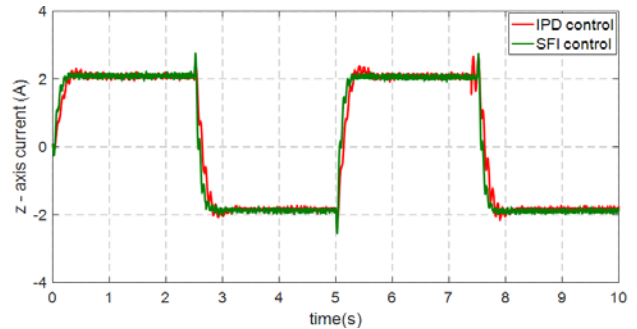


Fig. 15. Currents according to Z axis reference tracking.

In reference tracking, second and third experiments were conducted to observe axis response. ± 0.01 rad stepwise reference was applied to α and β axes respectively. I-PD and SFI controller trajectory tracking responses are shown in Fig. 16 and currents in Fig. 17 for α -axis, Figs. 18 and 19 for β -axis. Similar to z -axis experiment results, SFI controller outperforms I-PD controller in response time.

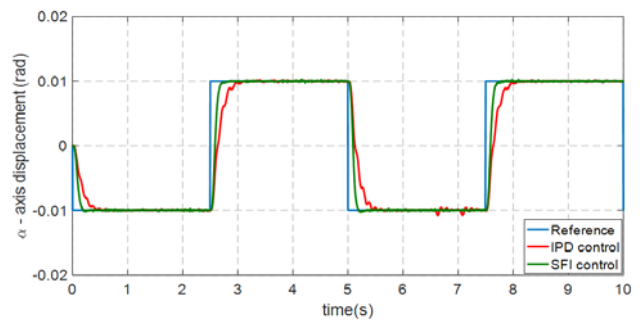


Fig. 16. $\pm 0.01\text{rad}$ reference tracking (α axis).

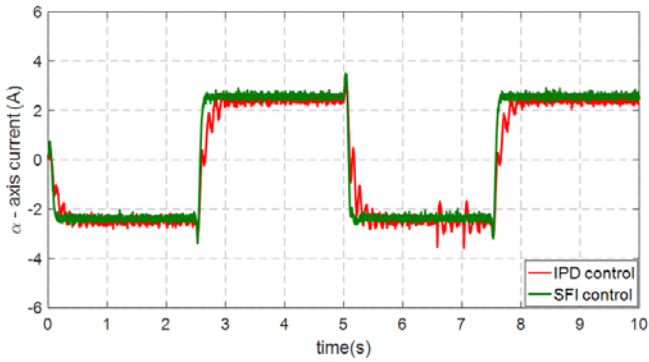


Fig. 17. Currents according to α axis reference tracking.

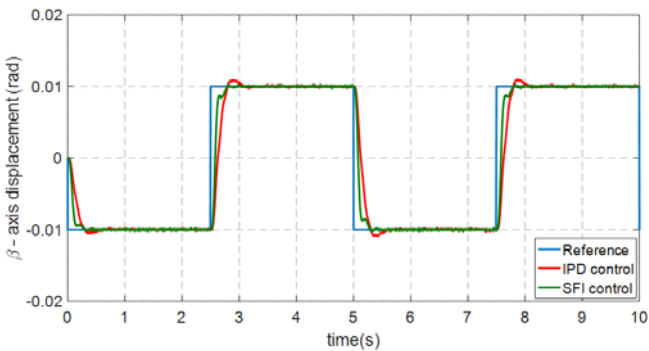


Fig. 18. ± 0.01 rad reference tracking (β axis).

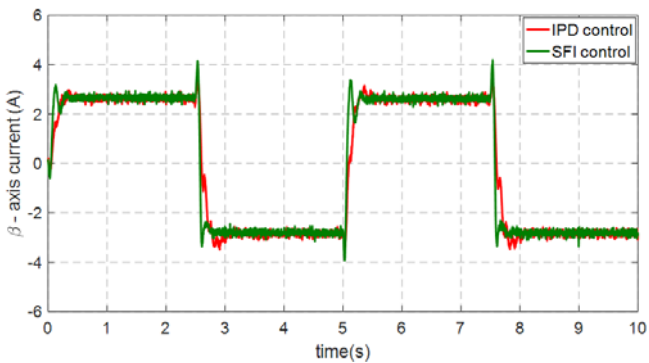


Fig. 19. Currents according to β axis reference tracking.

No overshoot is observed on the response α -inclination displacement for both SFI + DO and I-PD controllers. However, as seen in Fig. 17, I-PD results in considerably high oscillatory behavior which is unacceptable in practical sense because of high frequency components. Reference tracking performances of β -axis are almost identical except the overshoot seen for the I-PD controller. The current response depicted in Fig. 19 shows an oscillatory behavior for I-PD control. The proposed system is a mover that is supposed to convey a specified load one place to another. In practical applications, there would be changes in total mass, due to such a loading. The loading namely change of the levitation mass enters as an external disturbance to the system and degrades the performance and at the same time threatens its stability. If the load is applied on center, the levitation coils would draw the same current and z-axis current will be

increased; on the other hand, applying the load closer to the edges of the mover which corresponds to unbalanced loading causes increments/decrements on α -axis and/or β -axis currents. It is a must to test disturbance rejection on all axes in order to prove the robustness of the system. For this purpose, a 1.4 kg load was applied to the mover to induce unbalanced loading conditions at 3s of experimentation time and the load was removed at 8s time. The responses for disturbance test for each axis are given in Figs. 20 – 24. The responses reveal that the proposed control approach shows superior performance in terms of disturbance rejection. Especially, the effects of loading on displacements are remarkably smaller than that of I-PD controller. Furthermore, the settling time is relatively shortened and the current response is substantially less oscillatory.

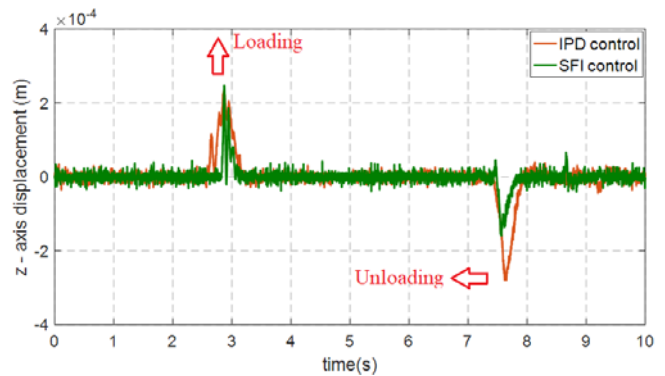


Fig. 20. Controllers compare on Z axis disturbance rejection.

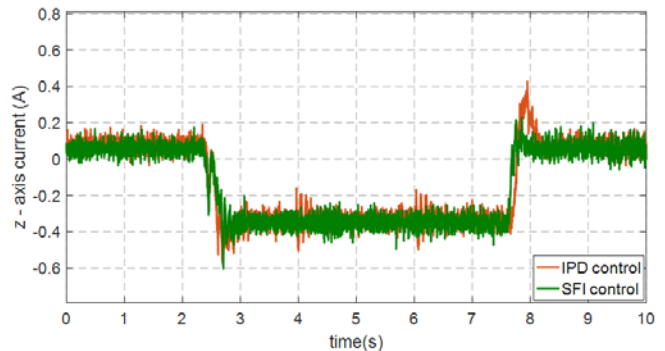


Fig. 21. Z axis disturbance effects on Z axis current.

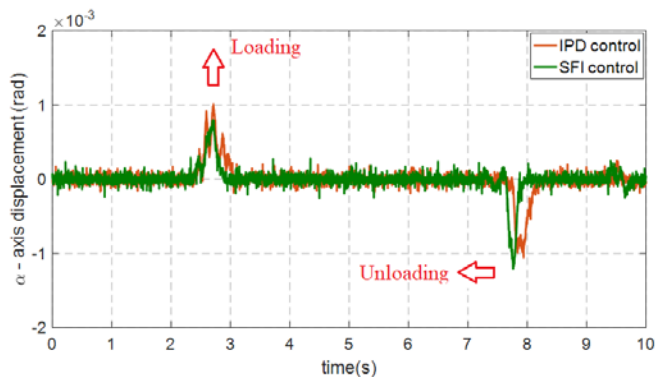


Fig. 22. Controllers compare on α axis disturbance rejection.

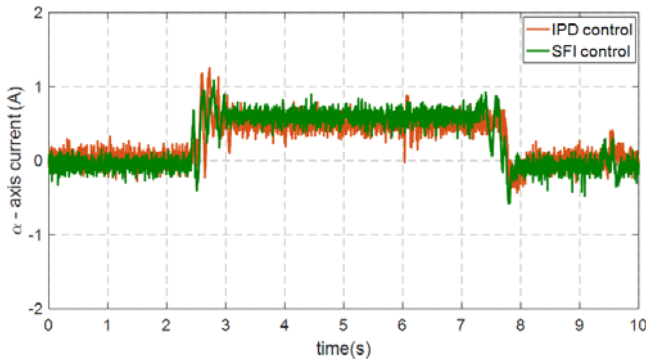


Fig. 23. α axis disturbance effects on α axis current.

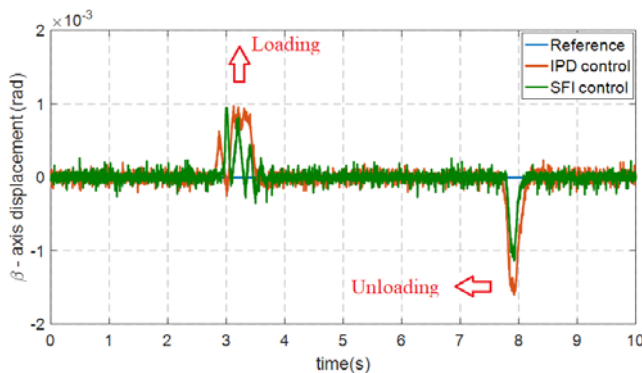


Fig. 24. Controllers compare on β axis disturbance rejection.

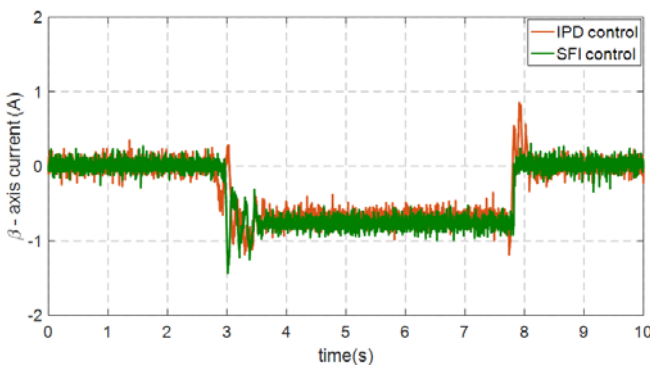


Fig. 25. β axis disturbance effects on β axis current.

5. CONCLUSION

In this paper, the novel maglev mover which consists of triple configuration of the hybrid electromagnet and linear motor units has been proposed. To develop and at the same time to clarify the effectiveness of the dynamic levitation model, 3D FEM analysis were carried out. As a result, it has been seen that the levitation dynamics can be decoupled from the linear motor dynamics and the analytical model representing the levitation dynamics has been obtained by employing well-established magnetic equivalent circuit approach. The model is non-linear in feature and unstable from the control point of view. To address the issue of instability and at the same time to enhance the levitation performance, SFI controller designs in the sense of centralized control was performed by using the linearized model of the mover in global axes via proper gap clearance and the current transformation matrices. SFI controller gains were obtained by using the canonical

polynomial approach of Manabe, relatively simple and effective method. The study is restricted to the availability of the gap clearance measurement and the associated displacement sensor. To complete the design of the SFI controller, DO usage has been proposed to estimate unmeasurable states. Therefore, the disturbance observer was designed and integrated into the SFI control loop. One of the most significant outcome of the DO is the accurate disturbance estimation. The estimated disturbance was properly scaled and feedforwarded to the control loop to compensate the undesired disturbance effects. To test and verify the proposed control approach, experimental studies were conducted on the test bench for reference tracking and disturbance rejection. Experimental results have shown that the proposed control approach has superior performance than I-PD control method in terms of reference tracking and disturbance rejection. I-PD control might be applicable, in case of the operating area confined around the linearization point with relatively small deviations.

ACKNOWLEDGEMENT

This work was supported by TUBITAK [grant number: 112M210] and YTU – BAP [grant number: 2013-06-04-KAP01]

REFERENCES

- Amrhein, W., Gruber, W., Bauer, W., Reisinger, M. (2016) "Maglev Systems for Cost-Sensitive Applications - Some Design Aspects", *IEEE Transactions on Industry Applications*, 52(5), 3739-3752.
- Baranowski, J., and Piątek, P. (2012) "Observer-based feedback for the magnetic levitation system", *Trans. of the Institute of Measurement & Control*, 34(4), 422-435.
- Barie W. and Chiasson J., (1996) "Linear & Nonlinear state-space controllers for magnetic levitation", *Int. Journal of Systems Science*, 27(11): pp. 1153-1163.
- Boldea, I. (2013), "*Linear Electric Machines, Drives, and Maglevs Handbook*", CRC Press.
- Bozkurt A.F., Erkan K., Güney Ö.F., (2015) "Zero Power Control of a 3-DoF Levitated Multiple Hybrid Electromagnet Flexible Conveyor System", *ACEMP-OPTIM-ELECTROMOTION*, Side, Turkey, pp. 570-575.
- Bucak, M., Bozkurt, A. F., Erkan, K., Üvet, H. (2017) "A new design concept of magnetically levitated 4 pole hybrid mover driven by linear motor", *IEEE Int. Conference on Robotics and Automation*, pp. 596-601.
- Choi, J.S., and Baek, Y.S. (2008) "Magnetically-Levitated Steel-Plate Conveyance System Using Electromagnets and a Linear Induction Motor", *IEEE Trans. on Magnetics*, 44(11): pp. 4171-4174.
- Erkan K., Acarkan B., Koseki T., (2007) "Zero-Power Levitation Control Design for a 4-Pole Electromagnet on the Basis of a Transfer Function Approach", *IEEE Int. Electric Machines & Drives Conference*, pp. 1751-56.
- Erkan K., Okur B., Koseki T., Yigit F., (2011) "Experimental evaluation of zero-power levitation control by transfer function approach for a 4-pole hybrid electromagnet", *IEEE Int. Conference on Mechatronics*, pp. 23-28.

- Erkan K., Yalçın B.C., Garip M., (2017) "Three-axis gap clearance I-PD controller design based on coefficient diagram method for 4-pole hybrid electromagnet", *Automatika*, 58(2): pp.147-167.
- Ertuğrul H., Erkan K., Üvet H., (2016) "Magnetic Levitation Control of A Three Degrees of Freedom 4-Pole Hybrid Electromagnet", *Journal of the Faculty of Engineering and Architecture of Gazi University*, 30(3): pp.631-643.
- Gottzein, E., Brock, K. H., Schneider, E., & Pfefferl, J. (1977). "Control aspects of a tracked magnetic levitation high speed test vehicle", *Automatica*, 13(3), 205-223.
- Gottzein, E., Meisinger, R., & Miller, L. (1980). "The Magnetic Wheel in the suspension of high-speed ground transportation vehicles", *IEEE Transactions on Vehicular Technology*, 29(1), 17-23.
- Güney Ö. F., Bozkurt A. F., Erkan K., (2017) "Centralized Gap Clearance Control for Maglev Based Steel-Plate Conveyance System", *Advances in Electrical and Computer Engineering*, 17(3): pp.101-106.
- Kim, C., Lee, J., Han, H., Kim, B. (2011) "Levitation and Thrust Control of a Maglev LCD Glass Conveyor", *IECON*, pp. 610-615.
- Kim C. H., Kim K. J., Yu J. S., Cho H. W., (2013) "Dynamic performance evaluation of 5-DOF maglev and guidance device by using equivalent magnetic circuit model", *IEEE Trans. on Magnetics.*, 49(7), pp. 4156- 4159.
- Kim, Y. H., Kim, K. M., Lee, J. (2001) "Zero power control with load observer in controlled-PM levitation", *IEEE Trans. on Magnetics*, 37(4): pp.2851-2854.
- Kubota F., Matsumoto S., Arai Y., Nakagawa T. (2013) "Control Techniques of Levitation and Guidance for Processing and Carrying Very Thin Steel Plates", *IECON*, pp. 3439-3444.
- Li, J. H. and Chiou, J. S. (2015) "GSA-tuning IPD control of a field-sensed magnetic suspension system", *Sensors*, 15(12): 31781-31793.
- Liu, C.T., Lin, S.Y., Yang, Y.Y. (2013) "Online Realizations of Dynamic Gap Detection and Control for Levitated Industrial Steel Plate Conveyance System", *IEEE Trans. on Industry Applications*, 49(5): pp. 1946-1953.
- Liu, J., Yakushi, K., Koseki, T. (2002) "Robust control of a 4-pole electromagnet in semi-zero-power levitation scheme with a disturbance observer", *IEEEJ Trans. on Industry Applications*, 122(1), 7-15.
- Makino, Y., Kovudhikulrungsri, L., Koseki, T. (2004) "6-DoF Control through Three Electromagnets and Three Linear Induction Motors", *Int. Symposium on Power Electronics, Electrical Drives, Automation Motion*.
- Manabe S., (1998) "Coefficient Diagram Method", *14th IFAC Symposium on Automatic Control in Aerospace*, Seoul.
- Manabe, S. (2002) "Application of Coefficient Diagram Method to MIMO design in aerospace", *IFAC Proceedings Volumes*, 35(1), 43-48.
- Matsumoto S., Arai Y., Nakagawa T. (2014) "Noncontact Levitation & Conveyance Characteristics of a Very Thin Steel Plate Magnetically Levitated by a LIM-Driven Cart", *IEEE Trans. on Magnetics*, 50(11): pp. 1-4.
- Morishita M., Azukizawa T., Kanda S., Tamura N., Yokoyama T., (1989) "A new Maglev system for magnetically levitated carrier system", *IEEE Trans. Veh. Technol.*, vol. 38, no. 4, pp. 230–236.
- Narita T., Oshinoya Y., Hasegawa S. (2011) "Study on Horizontal Non-contact Positioning Control for a Magnetically Levitated Thin Steel Plate", *Journal of Int. Council on Electrical Eng.*, 1(3): pp. 292-297.
- Sun Z.G., Cheung N.C., Zhao S.W., Gan W.C., (2009) "The Application of Disturbance Observer-based Sliding Mode Control for Maglev Systems", *Journal of Mechanical Eng. Science*, 224(8): pp. 1635-1644.
- Yang Z.J., Tsubakihara H., Kanae S., Wada K., Su C.Y., (2007) "Robust Nonlinear Control of a Voltage-Controlled Maglev System with Disturbance Observer", *16th IEEE Int. Conference on Control Applications*, Singapore, pp. 747-752.
- Yonezawa H., Narita T., Oshinoya Y., Marumori H., Hasegawa S. (2014) "Bending Magnetic Levitation Control for Thin Steel Plate", *IEEE Int. Power Electronics Conference*, pp. 3055-3060.